Research Paper

The Nrf2-inducers tanshinone I and dihydrotanshinone protect human skin cells and reconstructed human skin against solar simulated UV ☆

Shasha Tao [a], Rebecca Justiniano [a,b], Donna D. Zhang [a,b,*], Georg T. Wondrak [a,b,**]

[a] Department of Pharmacology and Toxicology, College of Pharmacy, University of Arizona, 1703 East Mabel Street, Tucson, AZ 85721, USA
[b] Arizona Cancer Center, University of Arizona, 1515 North Campbell Avenue, Tucson, AZ 85724, USA

ARTICLE INFO

ABSTRACT

Exposure to solar ultraviolet (UV) radiation is a causative factor in skin photocarcinogenesis and photoaging, and an urgent need exists for improved strategies for skin photoprotection. The redox-sensitive transcription factor Nrf2 (nuclear factor-E2-related factor 2), a master regulator of the cellular antioxidant defense against environmental electrophilic insult, has recently emerged as an important determinant of cutaneous damage from solar UV, and the concept of pharmacological activation of Nrf2 has attracted considerable attention as a novel approach to skin photoprotection. In this study, we examined feasibility of using tanshinones, a novel class of phenanthrenequinone-based cytoprotective Nrf2 inducers derived from the medicinal plant *Salvia miltiorrhiza*, for protection of cultured human skin cells and reconstructed human skin against solar simulated UV. Using a dual luciferase reporter assay in human Hs27 dermal fibroblasts pronounced transcriptional activation of Nrf2 by four major tanshinones [tanshinone I (T-I), dihydrotanshinone (DHT), tanshinone IIA (T-II-A) and cryptotanshinone (CT)] was detected. In fibroblasts, the more potent tanshinones T-I and DHT caused a significant increase in Nrf2 protein half-life via blockage of ubiquitination, ultimately resulting in upregulated expression of cytoprotective Nrf2 target genes (*GCLC*, *NQO1*) with the elevation of cellular glutathione levels. Similar tanshinone-induced changes were also observed in HaCaT keratinocytes. T-I and DHT pretreatment caused significant suppression of skin cell death induced by solar simulated UV and riboflavin-sensitized UVA. Moreover, feasibility of tanshinone-based cutaneous photoprotection was tested employing a human skin reconstruct exposed to solar simulated UV (80 mJ/cm^2 UVB; 1.53 J/cm^2 UVA). The occurrence of markers of epidermal solar insult (cleaved procaspase 3, pycnotic nuclei, eosinophilic cytoplasm, acellular cavities) was significantly attenuated in DHT-treated reconstructs that displayed increased immunohistochemical staining for Nrf2 and γ-GCS together with the elevation of total glutathione levels. Taken together, our data suggest the feasibility of achieving tanshinone-based cutaneous Nrf2-activation and photoprotection.

* Corresponding author at: University of Arizona, Department of Pharmacology and Toxicology, College of Pharmacy, 1703 East Mabel Street, Tucson, AZ 85721, USA. Tel.: +1 520 626 9918; fax: +1 520 626 2466.
** Corresponding author at: University of Arizona, Department of Pharmacology and Toxicology, College of Pharmacy, 1703 East Mabel Street, Tucson, AZ 85721, USA. Tel.: +1 520 626 0190; fax: +1 520 626 3797.
E-mail addresses: dzhang@pharmacy.arizona.edu (D.D. Zhang), wondrak@pharmacy.arizona.edu (G.T. Wondrak).

Introduction

The redox-sensitive transcription factor Nrf2 (nuclear factor-E2-related factor 2) has recently emerged as a promising molecular target for the pharmacological prevention of human pathologies resulting from exposure to environmental toxicants including poly-aromatic hydrocarbons (e.g. benzo[a]pyrene), polyhalogenated dioxins (e.g. 2,3,7,8-tetrachlorodibenzo-*p*-dioxin), metals (e.g. cadmium and arsenic), and electromagnetic radiation [including ionizing radiation and solar ultraviolet (UV) light] [1–10]. Nrf2 transcriptional activity orchestrates major cellular defense mechanisms including phase-II detoxification, inflammatory signaling, DNA repair, and antioxidant response thought to underlie tissue protection against electrophilic environmental insult [1,3,11,12].

Numerous natural products and dietary chemopreventive factors activate Nrf2 through covalent adduction and/or oxidation of redox-sensitive thiol residues in Keap1 (Kelch-like ECH-associated protein 1), the negative regulator of Nrf2 [3,11,13–15]. Inhibition of Keap1-dependent ubiquitination and subsequent proteasomal degradation

of Nrf2 allows nuclear translocation, a process followed by Nrf2-dependent transcriptional activation of cytoprotective target genes containing an antioxidant response element (ARE) regulatory sequence such as *GCLC* (glutamate-cysteine ligase catalytic subunit), *GCLM* (glutamate-cysteine ligase rmodifier subunit), *TXN* (thioredoxin), *PRDX1* (peroxiredoxin 1), *SRXN1* (sulfiredoxin 1), *NQO1* [NAD(P)H quinone oxidoreductase 1], and *HMOX1* (heme oxygenase-1) [3,11,14,15].

In an attempt to identify therapeutics for improved Nrf2-directed tissue protection against environmental insult we have recently focused our research on tanshinones, a novel class of phenanthrenequinone-based Nrf2-modulators derived from the medicinal plant *Salvia miltiorrhiza*. Based on their potent antioxidant, anti-inflammatory, and cytoprotective activities tanshinones [including tanshinone I (T-I), dihydrotanshinone (DHT), tanshinone IIA (T-II-A), and cryptotanshinone (CT); Fig. 1A] have recently emerged as experimental and clinically used phytotherapeutics showing efficacy in the prevention of cardiovascular disease, ischemia reperfusion injury, and hepatic fibrosis [16–18]. Recently, we have reported that T-I upregulates Nrf2-orchestrated gene expression protecting cultured human bronchial epithelial cells against electrophilic inflammatory insult imposed by the environmental toxicant arsenic [19]. In Nrf2 wild-type mice, systemic administration of T-I attenuated arsenic-induced inflammatory lung damage, a protective effect not observed in Nrf2 KO mice.

Exposure to solar UV-radiation is a causative factor in skin photocarcinogenesis and photoaging. Even though sunscreen-based broad spectrum photoprotection is an effective key component of a sun-safe strategy to reduce cumulative lifetime exposure to UV light, much effort has been directed towards the identification, development, and optimization of cutaneous photoprotectants that prevent and attenuate solar skin damage through mechanisms of action different from (or synergistic with) photon absorption [20–26]. Recent studies strongly suggest a protective role of Nrf2-mediated gene expression in the suppression of cutaneous photodamage induced by solar UV radiation, and Nrf2-activity has been identified as a functional determinant of UVA and UVB cytotoxicity in cutaneous keratinocytes and fibroblasts [5,6,27–33]. Importantly, Nrf2-dependent attenuation of UVB-induced sunburn reaction and oxidative DNA damage has been observed in Nrf2 wild-type compared to Nrf2 KO mice, and it has been demonstrated that UVB-induced photoaging is accelerated in Nrf2 KO mice as indicated by increased wrinkle formation, epidermal thickening, dermal deposition of extracellular matrix, lipid peroxidation, and loss of cutaneous glutathione [6,32,34]. Consequently, the concept of pharmacological activation of Nrf2 has attracted considerable attention as a novel approach to skin cell protection against solar damage but improved agents for Nrf2-directed skin cell photoprotection are needed [35].

In this study, based on the emerging role of Nrf2 activation in cutaneous defense against photodamage from solar UV and our previous identification of tanshinones as novel cytoprotective Nrf2 inducers, we examined feasibility of tanshinone-based skin photoprotection. We report for the first time that tanshinones are potent activators of the Nrf2-dependent cytoprotective response in cultured human skin keratinocytes and fibroblasts and that tanshinones protect cultured human skin cells and reconstructed human skin against cytotoxic doses of solar simulated UV radiation.

Materials and methods

Chemicals

Most chemicals including tanshinones (T-I, T-II-A, DHT, CT) were purchased from Sigma (St. Louis, MO). Sulforaphane (SF) was purchased from Santa Cruz (Santa Cruz, CA).
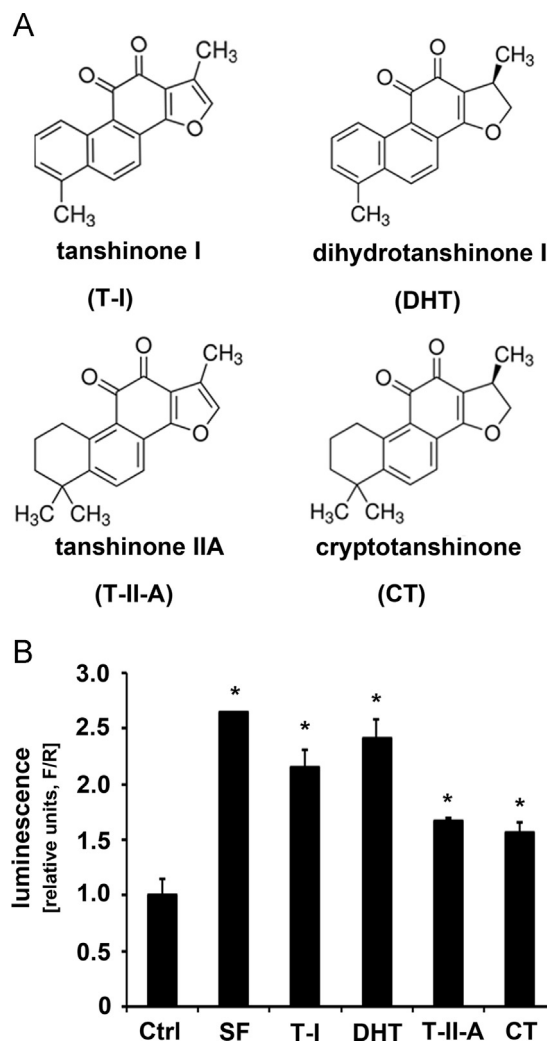

Fig. 1. Tanshinones, phenanthrenequinone-based natural products from the medicinal plant *Salvia miltiorrhiza*, cause Nrf2 transcriptional activation in human dermal fibroblasts. (A) Chemical structure of four major tanshinones [tanshinone I (T-I), dihydrotanshinone (DHT), tanshinone IIA (T-II-A), and cryptotanshinone (CT)]. (B) After transfection using an expression vector encoding an mGST-ARE firefly luciferase (F) reporter gene, human dermal Hs27 fibroblasts were exposed to test compounds (T-I, DHT, T-IIA, CT, SF; 5 μM; 16 h) or remained untreated. A plasmid encoding renilla luciferase (R) driven by the herpes simplex virus thymidine kinase promoter was included in all transfections to normalize transfection efficiency. Dual luciferase activities (R/F) were measured, and potency of fold induction is expressed as relative luminescence units (R/F) versus untreated control transfectants (mean ± SD, n=3; *p < 0.05).

Cell culture

Human dermal neonatal foreskin Hs27 fibroblasts from ATCC and human immortalized HaCaT keratinocytes were cultured in DMEM containing 10% fetal bovine serum. Cells were maintained at 37 °C in 5% CO_2, 95% air in a humidified incubator.

Reconstructed human skin

After shipment refrigerated EpiDerm™ Full Thickness inserts (EFT-400, 9 mm diameter; MatTek, Ashland, MA) were equilibrated in 6-well format (5% CO_2, 37 °C, 1 h; 0.9 ml of EFT-400-ASY media per well) followed by change of medium. Two days before UV exposure, EpiDerm™ tissues were treated by applying DHT [5 μM final concentration in EFT-400-ASY media] or EFT-400-ASY without DHT, followed by culture at 37 °C. Before irradiation, inserts were rinsed with PBS and then exposed in 6-well format

with 0.9 ml PBS in the well. After irradiation, PBS was removed and tissue inserts were cultured for another two days with daily change of media (EFT-400-ASY media with or without DHT, 5 μM). At the end of the incubation period, the tissues were rinsed and then fixed in neutral buffered formalin (10%, 24 h) and then placed in 70% ethanol followed by paraffin embedment and processing for H&E staining and immunohistochemical analysis.

Irradiation with solar simulated UV light (SSL) and UVA

A KW large area light source solar simulator, model 91293, from Oriel Corp. (Stratford, CT) was used, equipped with a 1000-W xenon arc lamp power supply, model 68920, and a VIS-IR band pass blocking filter plus either an atmospheric attenuation filter (output 290–400 nm plus residual 650–800 nm for solar simulated light) or UVB and UVC blocking filter (output 320–400 nm plus residual 650–800 nm, for UVA), respectively [36]. The output was quantified using a dosimeter from International Light Inc. (Newburyport, MA), model IL1700, with an SED240 detector for UVB (range 265–310 nm, peak 285 nm) or a SED033 detector for UVA (range 315–390 nm, peak 365 nm) at a distance of 365 mm from the source, which was used for all experiments. At 365 mm from the source, SSL dose was 7.63 mJ cm^{-2} s^{-1} UVA and 0.40 mJ cm^{-2} s^{-1} UVB radiation. Using a UVB/C-blocking filter, the dose at 365 mm from the source was 5.39 mJ cm^{-2} s^{-1} UVA radiation with a residual UVB dose of 3.16 μJ cm^{-2} s^{-1}.

Transfection of cDNA and luciferase reporter gene assay

Transfection of cDNA was performed using Lipofectamine 2000 (Invitrogen, Carlsbad, CA) used according to the manufacturer's instruction. Nrf2-dependent transcriptional activity was examined as previously published [37]. Hs27 fibroblasts were transfected with an mGST-ARE firefly luciferase reporter plasmid together with expression plasmids for Nrf2, Keap1, and renilla luciferase (internal control) using Lipofectamine 2000. At 24 h post-transfection, cells were treated with test compounds, and after 16 h cells were lysed for analysis of reporter gene activity. Reporter assays were performed using the dual-luciferase reporter gene assay system (Promega, Madison, WI). For each experiment all samples were run in triplicate, and the data represent the means of three independent repeats ± SD.

UV-impairment of skin cell viability

UV-induced toxicity was measured using the MTT [3-(4,5-dimethylthiazol-2-yl)-2,5-diphenyl tetrazolium bromide] assay. Briefly, cells (10,000 per well) were seeded on a 96-well plate and pretreated with test compounds (T-I, DHT, SF; 5 μM, 24 h) or solvent control (DMSO). Cells were then washed, placed under PBS (100 μL) and exposed to a dose range of SSL. Alternatively, cells were placed under PBS containing riboflavin (5 μM) and then exposed to a dose range of solar simulated UVA. After irradiation cell culture medium was added, and cells were cultured for another 24 h. For the analysis of survival, MTT (2 mg/ml; 20 μl; Sigma, St. Louis, MO) was directly added to the cells. After incubation (37 °C, 2 h), the plate was centrifuged and the medium was removed by aspiration. Isopropanol/HCl (100 μl) was added to each well with shaking at room temperature. Absorbance was then measured at 570 nm using the Synergy 2 Multi-Mode Microplate Reader (Biotek, Seattle, USA). All samples were run in triplicate for each experiment, and the data represent the means of three independent experiments.

Immunoblot analysis, ubiquitination assay, and determination of protein half-life

Antibodies for Nrf2 (sc-13032), Keap1 (sc-15246), NQO1 (sc-32793), γ-GCS (sc-55586) and GAPDH (sc-32233) were purchased from Santa Cruz (Santa Cruz, CA). Cells were harvested in sample buffer [50 mM Tris–HCl (pH 6.8), 2% SDS, 10% glycerol, 100 mM DTT, and 0.1% bromophenol blue]. After sonication, cell lysates were electrophoresed through an SDS–polyacrylamide gel and subjected to immunoblot analysis. For ubiquitination assay, Hs27 cells were co-transfected with expression vectors for HA-tagged ubiquitin and Nrf2, and after 24 h cells were then treated with SF, T-I or DHT (5 μM, each; 4 h) along with MG132 (10 μM) [38]. Cells were then harvested in buffer [2% SDS, 150 mM NaCl, 10 mM Tris–HCl (pH 8.0), 1 mM DTT] and immediately boiled. The lysates were then diluted fivefold in buffer lacking SDS and incubated with anti-Nrf2 antibody. Immunoprecipitated proteins were analyzed by immunoblotting using an antibody directed against the HA epitope (Santa Cruz). To measure Nrf2 protein half-life, Hs27 fibroblasts were either left untreated or treated with test compounds (DHT or T-I; 5 μM, 4 h). Cycloheximide (CHX, 50 μM) was added to block protein synthesis. Total cell lysates were collected at different time points and subjected to immunoblot analysis with anti-Nrf2 antibody. The relative intensity of the bands was quantified using the ChemiDoc CRS gel documentation system and Quantity One software from BioRad (Hercules, CA).

Real-time reverse transcription-polymerase chain reaction (RT-PCR)

RT-PCR was done on total mRNA extracted from cells using TRIZOL reagent (Invitrogen, Grand Island, NY). Equal amounts of mRNA were used to generate cDNA using the Transcriptor First Strand cDNA synthesis kit purchased from Roche (Roche, Indianapolis, IN). The PCR condition, Taqman probes and primers for h*NFE2L2* (Nrf2), *NQO1*, *GCLM*, and *GAPDH* were reported previously [19]. Briefly, Taqman probes were purchased from the universal probe library (Roche, Indianapolis, IN): h*NFE2L2* (#70), h*NQO1* (#87), h*GCLM* (#18), and h*GAPDH* (#25). Primers were synthesized by Sigma.

h*NFE2L2*: forward (acacggtccacagctcatc) and reverse (tgtcaatcaaatccatgtcctg);
h*NQO1*: forward (atgtatgacaaaggacccttcc) and reverse (tcccttgcagagagtacatgg);
h*GCLM*: forward (gacaaaacacagttggaacagc) and reverse (cagtcaaatctggtggcatc);
h*GAPDH*: forward (ctgacttcaacagcgacacc) and reverse (tgctgtagccaaattcgttgt).

The real-time PCR conditions used were the following: one cycle of initial denaturation (95 °C, 10 min), 40 cycles of amplification (95 °C, 10 s; 60 °C, 20 s), and a cooling period (50 °C, 5 s). Mean crossing point (Cp) values and standard deviations were determined. Cp values were normalized to the respective crossing point values of the h*GAPDH* reference gene. Data are presented as fold change in gene expression as compared to the control group. All quantitative RT-PCR data were generated in three independent experiments performed in duplicates. Data are all presented as means ± SD.

Detection of intracellular oxidative stress by flow cytometric analysis

Induction of intracellular oxidative stress by UVA/riboflavin photosensitization was analyzed by flow cytometry using 2′,7′-dichlorodihydrofluorescein diacetate (DCFH-DA) as a sensitive nonfluorescent precursor dye according to a published

standard procedure [22,23]. One hour after irradiation, DCFH–DA (5 µg/ml final concentration) was added to the culture medium and cells were incubated for 1 h in the dark (37 °C, 5% CO_2). Cells were harvested, washed with PBS, resuspended in 300 µl PBS and immediately analyzed by flow cytometry. To avoid direct photooxidation of the dye probe, cells were loaded with the indicator dye under light exclusion.

Glutathione assays

Total intracellular glutathione in cultured cells was analyzed using the QuantiChrom glutathione assay kit (BioAssay Systems) according to the manufacturer's instructions. The experiment was conducted in duplicates in three independent repeats. For glutathione determination in skin reconstructs, specimens first underwent epidermal–dermal separation and dispase-digest

(1 U/ml, 37ºC; sterile dispase I, from Bacillus polymyxa, Roche Applied Science) to recover keratinocytes from the epidermal portion following a standard procedure available from the manufacturer (EFT-400, MatTek, Corp.). Resuspended dissociated cells were counted using a Z2 Coulter counter, and GSH was determined per 10,000 viable cells using the ultrasensitive luminescent GSH-Glo™ glutathione assay (Promega, Madison, WI). Data represent relative levels of glutathione normalized for cell number comparing treated versus solvent controls (means ± SD; $n=3$).

Hematoxylin and eosin (H&E) staining and immunohistochemistry (IHC)

Reconstructed skin samples were stained using hematoxylin and eosin (H&E) according to standard procedures [39]. IHC analysis was performed as previously described. Following antigen retrieval, tissue
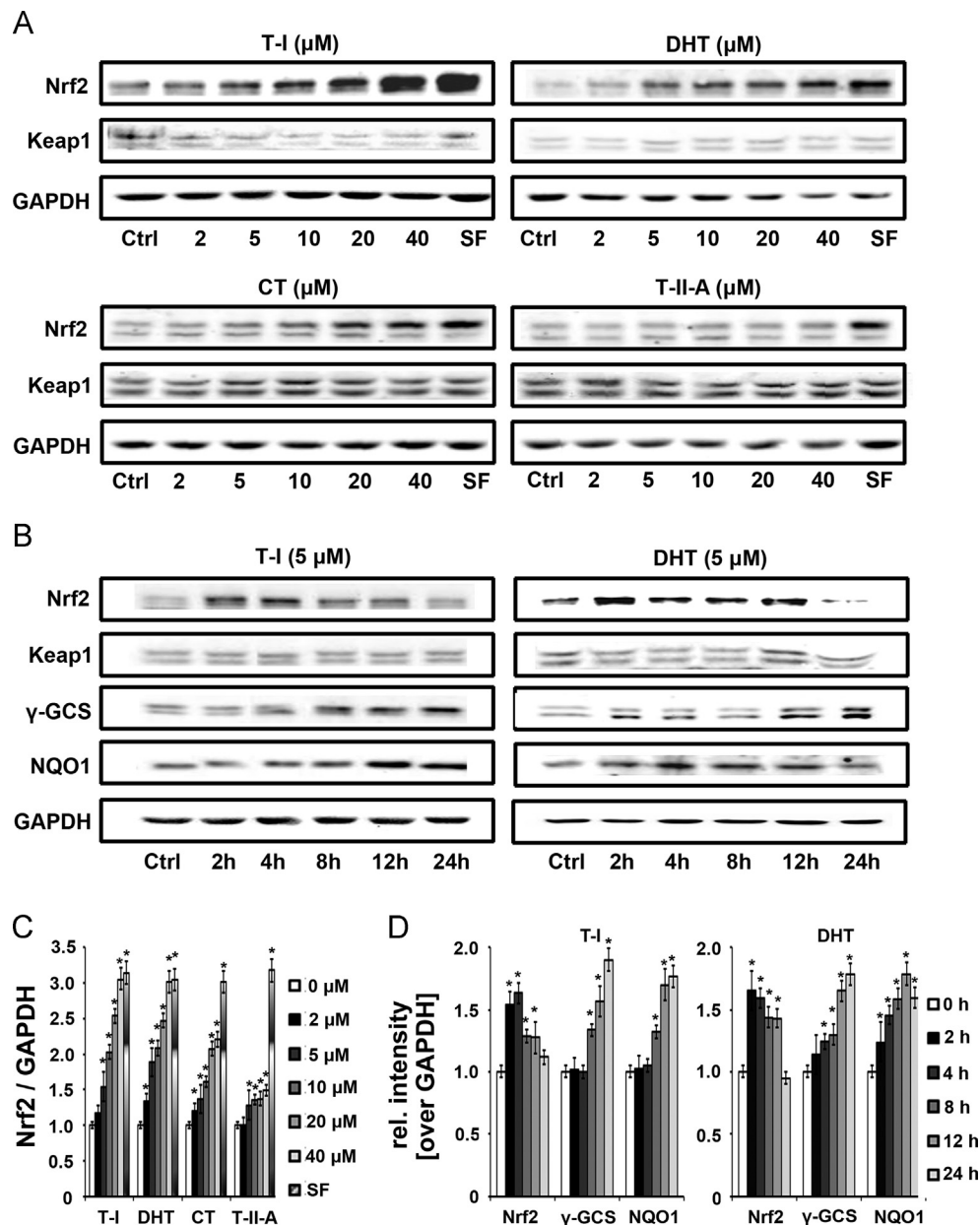

Fig. 2. Tanshinone I and dihydrotanshinone upregulate protein levels of Nrf2 and Nrf2 targets in human dermal fibroblasts. (A) Dose–response relationship of tanshinone-induced the upregulation of Nrf2 protein levels. Hs27 fibroblasts were exposed to four types of tanshinones (T-I, DHT, T-IIA, CT; 5 µM, each; 4 h) followed by immunoblot analysis. SF (5 µM; 4 h) treatment was included as a positive control. (B) Time course of tanshinone-induced the upregulation of Nrf2, NQO1, and γ-GCS. Hs27 fibroblasts were exposed to tanshinones (T-I, DHT; 5 µM, 2–24 h) and total cell lysates were subjected to immunoblot analysis. Detection of GAPDH served as a loading control. (C) Quantitative analysis of triplicate gels as presented in panel A. (D) Quantitative analysis of triplicate gels as presented in panel B. Relative intensity of protein bands was determined using gel documentation software as described in "Materials and methods" (mean ± SD, $n=3$; *$p < 0.05$).

sections were incubated with 5% normal goat serum for 30 min followed by 2 h incubation using the respective antibodies [Nrf2, γ-GCS (as described above), cleaved caspase 3 (Asp175; 9664, Cell Signaling, Danvers, MA)] [23]. Sections were incubated with a biotinylated secondary antibody. The ABC kit (Vector Laboratories, Burlingame, CA) was then used according to the manufacturer's instructions. Tissue sections were developed using the 3,3′-diamino-benzidine staining kit (DAKO, Carpinteria, CA), and counterstained with hematoxylin.

Statistics

All the results are presented as the means $\pm$ SD of at least three independent experiments performed in duplicate or triplicate each.

Data were analyzed employing the two-sided Student's t-test; differences were considered significant at $p < 0.05$ (*$p < 0.05$; **$p < 0.01$; ***$p < 0.001$). Selected data sets were analyzed employing one-way analysis of variance (ANOVA) with Tukey's post hoc test using the PRISM 4.0 software; means without a common letter differ ($p < 0.05$).

Results

Identification of tanshinone I and dihydrotanshinone as potent Nrf2-inducers in human dermal fibroblasts

In an attempt to explore the Nrf2-based cytoprotective potential of tanshinones against environmental exposure we aimed at
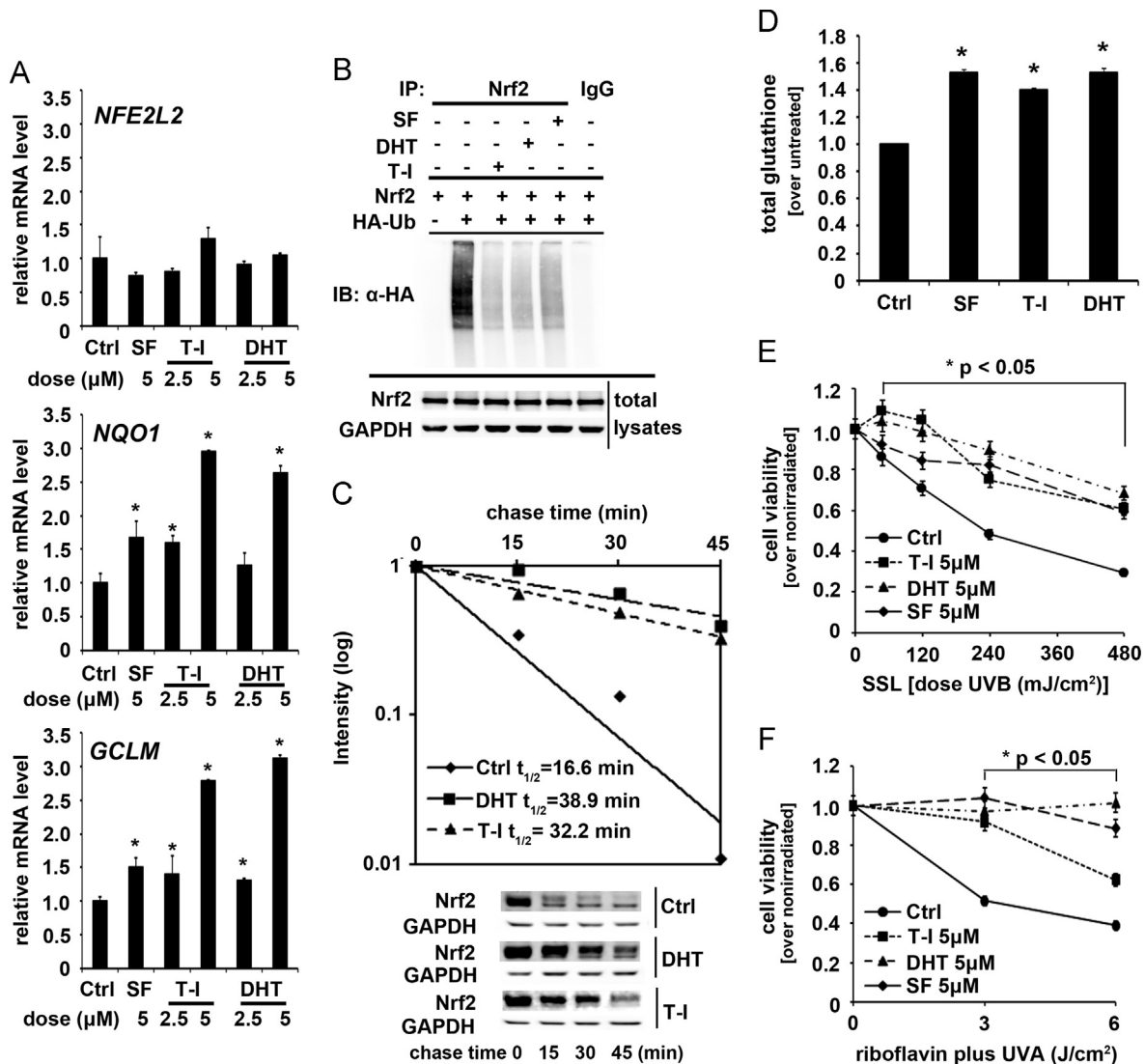

Fig. 3. Tanshinones increase Nrf2 half-life via interference with ubiquitination, elevate intracellular glutathione, and protect dermal fibroblasts against UV-induced cytotoxicity. (A) Tanshinone-modulation of Nrf2 and Nrf2 target gene expression. Hs27 Fibroblasts were treated with T-I and DHT (5 μM; 16 h) and mRNA was extracted. The relative mRNA levels of Nrf2 and its downstream genes (NQO1, GCLM) were determined by quantitative real-time RT-PCR with triplicate samples in each experiment. The experiment was conducted in triplicate and expressed as mean $\pm$ SD (*$p < 0.05$). (B) Tanshinone-modulation of Nrf2-ubiquitination. Hs27 cells were co-transfected with plasmids encoding the indicated proteins (Nrf2, HA-Ub). Cells were then treated with SF, T-I or DHT (5 μM; 4 h) along with MG132 (10 μM; 4 h) before cell lysates were collected for the ubiquitination assay. For the detection of ubiquitin-conjugated Nrf2, anti-Nrf2 immunoprecipitates were analyzed by immunoblotting using an anti-HA antibody. (C) Tanshinone-modulation of Nrf2 protein half-life. Hs27 cells were left untreated or treated with T-I or DHT (5 μM; 4 h). Cycloheximide (50 μM) was added and cells were harvested at the indicated time points (0–45 min). Cell lysates were subjected to immunoblot analysis using anti-Nrf2 and anti-GAPDH antibodies. The intensity of the bands was quantified using Quantity One software and plotted against the time after cycloheximide treatment. (D) Intracellular total glutathione levels relative to untreated control were determined in fibroblasts exposed to tanshinones (T-I, DHT) or SF (5 μM, each; 24 h) using the QuantiChrom glutathione assay kit as detailed in Materials and Methods. (E and F) To assess cytoprotective effects of tanshinone treatment on UV-induced cytotoxicity, fibroblasts were first preincubated in the presence of T-I or DHT (5 μM; 24 h) and then exposed to full spectrum solar simulated UV [solar simulated light (SSL); panel E] or solar simulated UVA delivered in the presence of the photosensitizer riboflavin [5 μM (UVA+riboflavin); panel F], followed by assessment of cell viability at 24 h post-irradiation. Data are expressed as means $\pm$ SD (*$p < 0.05$; $n=3$).

testing selected tanshinones for skin cell photoprotection against solar UV radiation. To this end, potency of transcriptional activation of Nrf2 in Hs27 human dermal fibroblasts was compared among four major tanshinones (T-I, DHT, T-II-A, CT) using a dual luciferase reporter assay employing an mGST-ARE firefly luciferase plasmid (Fig. 1B). Exposure to tanshinone test compounds caused a significant 1.5–2.5-fold upregulation of Nrf2 transcriptional activity over untreated controls, and T-I or DHT were significantly more potent than T-II-A or CT (5 μM, each), with DHT causing a similar degree of induction as an equimolar dose of the isothiocyanate-based Nrf2 inducer sulforaphane (SF).

Next, tanshinone-induced Nrf2 activation was examined at the protein level employing immunoblot analysis (Fig. 2). Fibroblasts were exposed to a dose range of test compounds (T-I, DHT, T-II-A, CT; 2–40 μM; 4 h), and modulation of cellular Nrf2 protein levels was examined. As already observed by luciferase-based assessment of Nrf2 transcriptional activity (Fig. 1B), all tanshinones caused an increase in Nrf2 protein levels in a dose-dependent manner, whereas no effects were observed on Keap1 protein levels. T-I or DHT were significantly more potent than CT or T-II-A, upregulating Nrf2 levels at concentrations equal or above 2 μM (Fig. 2A and C). CT displayed attenuated activity, upregulating Nrf2 protein levels only at concentrations equal or above 10 μM, and T-II-A displayed only minimal activity.

Next, time course analysis of Nrf2 modulation by T-I or DHT (5 μM; 2–24 h) was conducted monitoring protein levels of Nrf2 and Nrf2 targets (NQO1, γ-GCS) (Fig. 2B and D). A significant increase in Nrf2 protein level was observable at early time points (2 h) and persisted for up to 12 h for both tanshinones, whereas no changes were observed with Keap1 protein levels (Fig. 2B). At later time points Nrf2 protein levels returned to basal levels, whereas protein levels of the Nrf2 target proteins displayed sustained upregulation (24 h). Based on the appreciable Nrf2 activation displayed by T-I and DHT that surpassed that of T-II-A and CT, we pursued further experimentation focusing on T-I and DHT.

Tanshinones increase Nrf2 protein half-life via blockage of ubiquitination, elevating intracellular glutathione and protecting dermal fibroblasts against solar UV-induced cytotoxicity

After examining dose–response relationship and time course of tanshinone-induced modulation of Nrf2 at the protein level, we examined Nrf2 mRNA levels in tanshinone treated cells. However, no changes were observed in response to either tanshinones (T-I, DHT; 5 μM; 16 h) or the standard Nrf2 inducer SF (5 μM; 16 h) (Fig. 3A). In contrast, exposure to T-I or DHT upregulated expression of Nrf2 target genes (NQO1 and GCLM) at the mRNA level by up to threefold, an induction equal or superior to that observed in response to SF (Fig. 3A). Taken together these data indicate that in dermal fibroblasts T-I and DHT activate the Nrf2 pathway by upregulation of Nrf2 at the protein level.

Next, we investigated the molecular mechanism underlying Nrf2 activation by T-I and DHT in more detail. As demonstrated previously, established Nrf2 inducers such as SF and tBHQ cause Nrf2 activation through inhibition of the Keap1-mediated ubiquitination of Nrf2 [40]. Therefore a cellular ubiquitination assay was performed using Hs27 fibroblasts co-transfected with expression vectors for Nrf2 and hemagglutinin (HA)-ubiquitin, followed by immunoprecipitation of Nrf2 and immunodetection of ubiquitinated protein using an anti-HA antibody. After transfection, cells were either left untreated or exposed to T-I, DHT, or SF. In cells treated with T-I or DHT (5 μM; 4 h), ubiquitination of Nrf2 decreased dramatically compared to untreated control (Fig. 3B). As expected, SF (5 μM; 4 h) also decreased Nrf2 ubiquitination (Fig. 3B). Next, the half-life of endogenous Nrf2 protein was measured. Cycloheximide (CHX) was added to either untreated

or tanshinone-exposed Hs27 fibroblasts (5 μM; 4 h pretreatment) followed by quantitative determination of Nrf2 by immunoblot analysis (Fig. 3C, right panel). Intensity of Nrf2 bands was determined densitometrically and plotted as a function of time after addition of CHX, and the half-life of Nrf2 was calculated (Fig. 3C, left panel). The half-life of Nrf2 under untreated conditions (control) was 16.6 min, whereas Nrf2 half-life almost doubled (32.2 min) following T-I treatment and was increased more than 2.3-fold (38.9 min) in response to DHT treatment (5 μM, each). Taken together, these results indicate that T-I and DHT induce the Nrf2-dependent stress response in dermal fibroblasts by decreasing Nrf2 ubiquitination causing stabilization of Nrf2 at the protein level.

Next, we tested feasibility of raising cellular glutathione levels by tanshinone treatment in dermal fibroblasts (Fig. 3D). Indeed, intracellular concentrations of total glutathione were significantly increased by approximately 35–40% over untreated control cells when fibroblasts were exposed to tanshinones (T-I or DHT, 5 μM; 24 h), a finding consistent with Nrf2-dependent upregulation of GCLM mRNA and ©-GCS protein levels as detailed above (Figs. 2 B and 3A). Again, as observed with modulation of Nrf2 protein half life (Fig. 3C), DHT was slightly more efficacious than T-I causing a similar increase of cellular glutathione content as observed in response to treatment with SF (5 μM; 24 h) used as a reference Nrf2-inducer (Fig. 3D).

Earlier research has demonstrated that Nrf2-dependent upregulation of intracellular glutathione is a key factor mediating photoprotective effects of Nrf2 against solar UV-induced skin cell damage [5]. After demonstrating tanshinone-induced Nrf2 activation and modulation of cellular glutathione status, we therefore assessed cytoprotective effects of tanshinone preincubation on UV-induced cytotoxicity in dermal fibroblasts (Fig. 3E and F). Cells were first preincubated in the presence of T-I or DHT (5 μM; 24 h) and then exposed to a broad dose range of either full spectrum solar simulated UV [UVA plus UVB; solar simulated light (SSL); Fig. 3E], followed by assessment of cell viability at 24 h post-irradiation. In addition, exposure to solar simulated UVA was employed. Specifically, UVA was delivered in the presence of the photosensitizer riboflavin [vitamin B₂, 5 μM (UVA+riboflavin); Fig. 3F], an accepted model of UVA-induced photooxidative stress enhanced by inclusion of an endogenous UVA-photosensitizer [41,42]. As a positive control, photoprotective activity of SF, shown earlier to suppress skin cell photodamage in response to solar UV exposure, was also assessed [6,29,35]. Remarkably, tanshinone (T-I, DHT) pretreatment significantly attenuated SSL-induced loss of fibroblast viability, increasing the proportion of cells surviving apoptogenic doses of SSL (up to 9.2 J/cm² UVA plus 480 mJ/cm² UVB; Fig. 3E) more than twofold. Equally, significant suppression of riboflavin-enhanced UVA phototoxicity (UVA doses up to 6 J/cm²), was observed when cells received either T-I or DHT pretreatment (Fig. 3F). Protection against SSL-induced cytotoxicity did not differ between T-I- and DHT-treated cells, but DHT was significantly more potent than T-I protecting fibroblasts against riboflavin-enhanced UVA phototoxicity. Taken together, these data indicate feasibility of tanshinone-based Nrf2-activation, glutathione upregulation, and solar photoprotection of dermal fibroblasts.

Tanshinone-based Nrf2 activation protects HaCaT keratinocytes and reconstructed human skin against solar UV-induced cytotoxicity

Next, human HaCaT keratinocytes were exposed to a dose range of tanshinones (T-I and DHT; 2.5–20 μM; 4 h), and modulation of Nrf2 protein levels was monitored by immunoblot analysis (Fig. 4A). Pronounced upregulation of Nrf2 protein levels was observed at low micromolar concentrations (T-I: 2.5 and 5 μM; DHT: 2.5 μM), similar to that induced by SF (5 μM; 4 h). Next, a
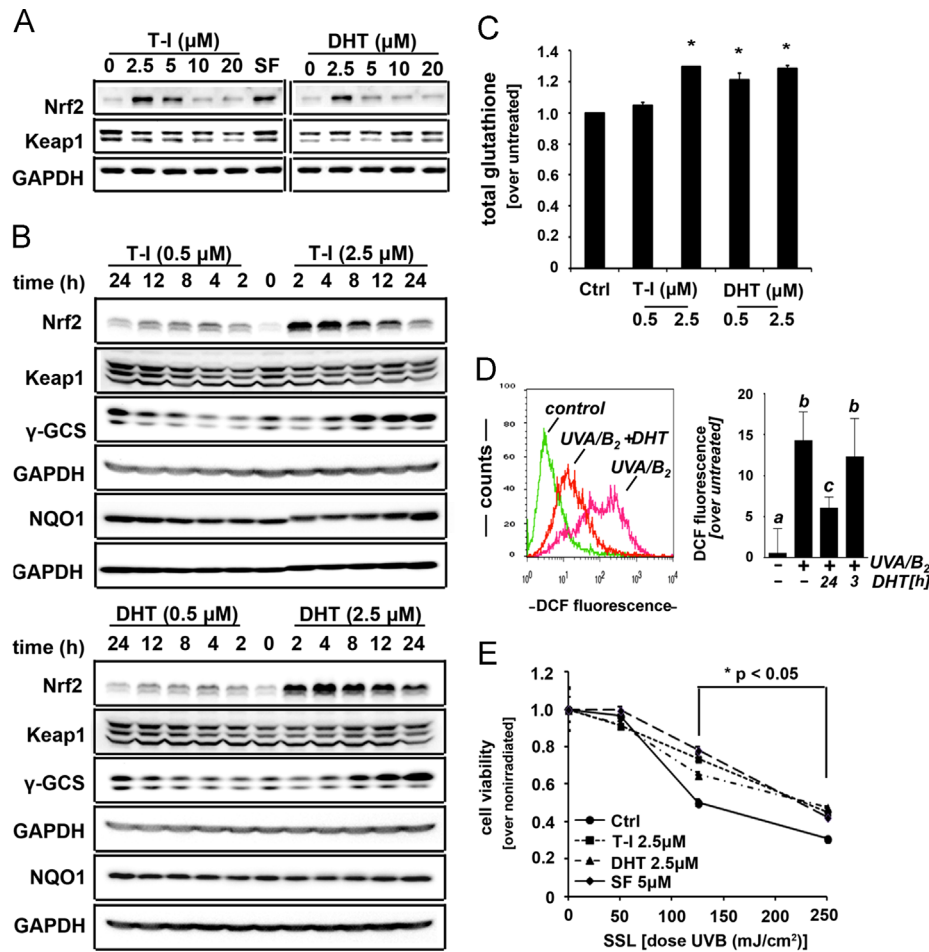
Fig. 4. Tanshinones activate Nrf2 in HaCaT keratinocytes and reconstructed human skin providing protection against solar UV-induced cytotoxicity. (A) Dose–response relationship of tanshinone-induced upregulation of Nrf2 protein levels. HaCaT cells were exposed to tanshinones (T-I, DHT; 5 μM, each; 4 h) followed by immunoblot analysis. SF (5 μM; 4 h) treatment was included as a positive control. Detection of GAPDH served as a loading control. (B) Time course of tanshinone-induced modulation of Nrf2, Keap1, γ-GCS, and NQO1. HaCaT cells were exposed to tanshinones (T-I, DHT; 0.5 and 2.5 μM, 2–24 h), and total cell lysates were subjected to immunoblot analysis. Detection of GAPDH served as a loading control. In addition, NQO1 samples are shown with their own GAPDH loading control. (C) Intracellular total glutathione levels relative to untreated control were determined in HaCaT cells exposed to tanshinones (T-I, DHT; 0.5 and 2.5 μM) using the QuantiChrom glutathione assay kit as detailed in "Materials and methods". (D) Modulation of cellular oxidative stress was examined in cells preincubated in the absence or presence of DHT (2.5 μM; 3 or 24 h preincubation time) followed by exposure to the combined action of UVA (1.5 J/cm^2) and vitamin B$_2$ (5 μM). One hour after irradiation flow cytometric detection of DCF fluorescence was performed. One representative histogram is shown (control versus UVA/B$_2$ versus UVA/B$_2$+DHT (24 h, preincubation). Bar graph depicts summary data of at least three independent repeats ($n \geq 3$, mean $\pm$ SD). Data were analyzed employing one-way analysis of variance (ANOVA) with Tukey's post hoc test. Means without a common letter differ ($p < 0.05$). (E) Cytoprotective effects of tanshinone treatment on UV-induced cytotoxicity. HaCaT cells were first preincubated in the presence of T-I or DHT (2.5 μM; 24 h) and then exposed to full spectrum solar simulated UV [solar simulated light (SSL); upper panel] followed by assessment of cell viability at 24 h post-irradiation. Data are expressed as means $\pm$ SD ($^*p < 0.05$; $n=3$).

time course analysis of Nrf2 modulation by T-I or DHT was conducted (Fig. 4B). Exposure to T-I or DHT (2.5 μM, each) caused a rapid increase in Nrf2 protein levels within 2 h exposure time detectable for up to 12 h, and Nrf2 upregulation occurred at concentrations as low as 0.5 μM (Fig. 4B). At 24 h Nrf2 protein levels almost returned to basal levels, but protein levels of Nrf2 downstream targets (NQO1, γ-GCS) displayed sustained upregulation even at later time points (24 h; Fig. 4B). In contrast, Keap1 protein levels remained unchanged over 24 h exposure time.

Next, feasibility of raising cellular glutathione levels in response to tanshinone exposure was tested in HaCaT keratinocytes. Consistent with Nrf2-dependent upregulation of total cellular glutathione as observed in tanshinone-exposed dermal fibroblasts (Fig. 3D), glutathione levels in HaCaT keratinocytes were significantly increased by up to 30% over untreated controls in response to exposure to T-I or DHT (2.5 μM, 24 h; Fig. 4C).

Next, we assessed the protective effects of tanshinone preincubation on UVA-induced photooxidative stress in HaCaT keratinocytes (Fig. 4D). To this end, cells were first preincubated in the absence or presence of DHT (2.5 μM; 3 or 24 h preincubation time), followed by exposure to the combined action of UVA and vitamin B$_2$. Cellular oxidative stress was then assessed 1 h after irradiation employing flow cytometric detection of DCF fluorescence. Indeed, DHT preincubation efficiently suppressed UVA/B$_2$-induced photooxidative stress causing an almost threefold suppression of UVA/B$_2$-induced DCF fluorescence intensity. Remarkably, this effect was only observed if DHT preincubation occurred during an extended period of time (24 h) whereas short term preincubation (3 h) was not sufficient to protect cells against UVA-induced photooxidative stress, a finding consistent with DHT acting through Nrf2-dependent biological upregulation of cellular antioxidant defenses (e.g. biosynthesis of glutathione) rather than through direct antioxidant chemical reactivity.

Next, tanshinone-based [T-I or DHT (2.5 μM; 24 h)] photoprotection of HaCaT keratinocytes was examined employing a dose range of full spectrum solar simulated UV [SSL], followed by assessment of cell viability at 24 h post-irradiation (Fig. 4E). As a positive control, photoprotective activity of the standard Nrf2-inducer SF was also
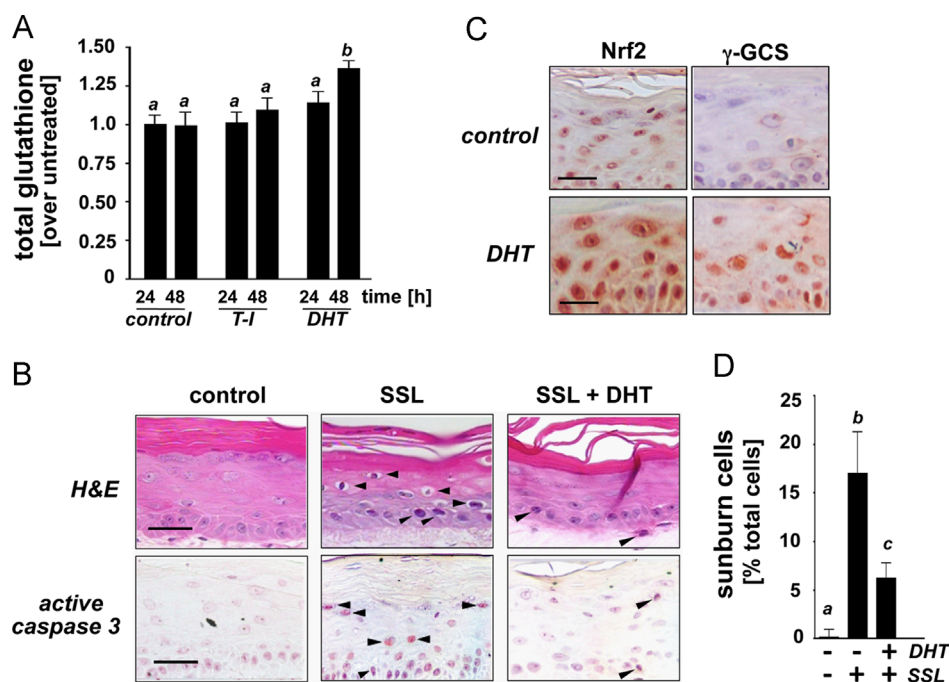
Fig. 5. Tanshinone-based cutaneous Nrf2 activation, glutathione upregulation, and protection against solar UV exposure. (A) Elevation of total cellular glutathione levels in keratinocytes from skin specimens cultured in growth medium supplemented with tanshinones (DHT or T-I, 5 μM each; 24 and 48 h exposure; $n \geq 3$; mean ± SD) or cultured in based medium without supplementation. After culture, keratinocytes were retrieved from skin reconstructs by dispase-digest, and glutathione levels were normalized to cell number. (B) Two days before SSL (80 mJ/cm^2 UVB; 1.53 J/cm^2 UVA) exposure, growth medium was supplemented with DHT (5 μM), whereas control reconstructs remained untreated. (C) Upregulation of Nrf2 and γ-GCS was examined by immunohistochemical analysis of human skin reconstructs after exposure to growth medium supplemented with DHT (5 μM, each; 48 h). Controls remained untreated; scale bar=25 μm. Two days after SSL exposure reconstructs were harvested and processed for IHC. Arrowheads indicate localization of photodamaged keratinocytes (H&E: pycnotic nuclei, eosinophilic cytoplasm, loss of cellularity; IHC: cleaved procaspase 3; scale bar=50 μm). Per treatment group representative images taken from three independent repeat samples are displayed. (D) The bar graph displays quantitative analysis of keratinocyte photodamage [percentage of sunburn cells per high power field; at least three independent skin reconstructs per group (mean ± SD); one-way analysis of variance (ANOVA) with Tukey's post hoc test]. Means without a common letter differ ($p < 0.05$).

assessed. As observed before with dermal fibroblasts (Fig. 3E), tanshinone (T-I, DHT) pretreatment significantly attenuated SSL-induced loss of keratinocyte viability, increasing the proportion of cells still viable after receiving apoptogenic doses of SSL (up to 4.8 J/cm^2 UVA plus 250 mJ/cm^2 UVB) by approximately 50%. Differences in protective efficacy against SSL-induced cytotoxicity between T-I- and DHT-treated cells did not reach the level of statistical significance.

Next, feasibility of tanshinone-based cutaneous photoprotection was tested directly using an organotypic model of human skin (Fig. 5). A full thickness human skin reconstruct with differentiated viable epidermis was employed. First, the effect of tanshinone exposure on epidermal glutathione levels was examined, and tanshinone-induced upregulation of Nrf2 and the Nrf2-target γ-GCS was monitored. To this end, growth medium was supplemented with T-I or DHT (5 μM, each; 24 and 48 h), and control reconstructs remained untreated (Fig. 5A). Following enzymatic (dispase-dependent) recovery of viable keratinocytes from the epidermis elevation of total glutathione levels was observable in DHT exposed skin specimens, an effect that reached the level of statistical significance upon prolonged exposure (48 h) displaying an approximately 1.25-fold increase over untreated control specimens. Since DHT caused a more pronounced elevation of epidermal glutathione than T-I, the subsequent skin photoprotection experiment employed DHT as experimental Nrf2 inducer. Indeed, DHT-induced upregulation of Nrf2 and γ-GCS protein levels was confirmed by immunohistochemical (IHC) analysis (Fig. 5B). In response to DHT exposure pronounced nuclear localization of Nrf2 and increased expression levels of γ-GCS were observed. Next, feasibility of achieving DHT-induced skin photoprotection against solar UV was tested. To this end, solar UV insult was caused by exposure of reconstructed human skin to SSL (80 mJ/cm^2 UVB; 1.53 J/cm^2 UVA), delivering a UVB dose shown earlier to impair keratinocyte viability and to disrupt structural integrity of reconstructed human skin with sunburn cell formation and caspase 3 activation [43,44]. Two days before exposure, growth medium was either supplemented daily with DHT (5 μM) or remained unsupplemented. Two days after irradiation reconstructs were harvested, and occurrence of keratinocyte photodamage was examined by H&E staining and immunohistochemical visualization of cleaved procaspase 3 (active caspase 3; Fig. 5C and D). Strikingly, H&E staining revealed the occurrence of tissue damage in response to SSL exposure as obvious from (i) the presence of pycnotic nuclei with eosinophilic cytoplasmic staining ("sunburn" cells), (ii) the occurrence of acellular cavities indicative of massive loss of epidermal cellularity, and (iii) reduced epidermal thickness, consistent with UV-induced cell death and inhibition of proliferation that impair epidermal growth and viability over the three-day post-irradiation period [43,44]. Moreover, staining for cleaved procaspase 3 (activated caspase 3), a hallmark of UV-induced epidermal photodamage, was detectable in keratinocytes of reconstructed human skin exposed to SSL (Fig. 5C), a finding consistent with published research that has documented caspase 3 cleavage in epidermal keratinocytes of reconstructed human skin exposed to UVB, delivered at doses comparable to the one used in this study [43]. In contrast, the occurrence of markers of solar damage was significantly attenuated in SSL-exposed DHT-treated reconstructs, that displayed a significant almost threefold reduction in the number of sunburn cells (Fig. 5C and D) and an approximately twofold reduction in the number of caspase 3 positive nuclei (Fig. 5C; numerical analysis not depicted). These observations demonstrate feasibility of protecting reconstructed human skin against solar UV-induced loss of keratinocyte viability using the tanshinone DHT that upregulates Nrf2 and cytoprotective Nrf2 targets including glutathione.

Discussion

Exposure to chronic solar UV-radiation is a causative factor underlying cutaneous photocarcinogenesis and photoaging. The importance of efficient skin UVB (290–320 nm) photoprotection that attenuates photomutagenic events originating from direct absorption of UVB photons by DNA bases is firmly established as reviewed recently [20,21,23,45]. In addition, cumulative evidence for the involvement of chronic UVA exposure in the causation of solar skin damage, thought to occur through photooxidative mechanisms mediated by reactive oxygen species (ROS), now dictates the necessity for additional broad spectrum skin photoprotection that includes the UVA spectral region of sunlight [25,46]. Significant research has focused on the identification of molecular interventions and agents designed to provide synergistic photoprotective benefit if used together with sunscreen application (referred to as "non-sunscreen photoprotection") as reviewed previously [26,47–52].

Recently, pharmacological activation of Nrf2 has been explored as a novel strategy for skin cell photoprotection, and a limited number of prototype agents has shown efficacy [6,28,29,33,35,53,54]. Specifically, It has been shown earlier that pharmacological Nrf2-activation by topical administration of the Nrf2 inducer sulforaphane suppresses UVB-induced acute inflammation and sunburn reaction in murine skin [6], and topical application of broccoli sprout extracts containing sulforaphane protected against UVB-induced skin carcinogenesis in SKH1 hairless mice [28], but the photochemopreventive activity of topical sulforaphane application has also been attributed to potent inhibition of AP-1 [55]. Moreover, the small molecule Nrf2 activator cinnamaldehyde displayed strong cytoprotective activity by suppressing reactive oxygen species (ROS)-dependent photooxidative stress in cultured skin keratinocytes and fibroblasts [53], and the photoprotective potential of a synthetic tricyclic bis(cyanoenone)-based Nrf2 inducer has been substantiated by demonstrating suppression of UVA-induced skin photooxidative stress in a murine model of systemic immunomodulatory thiopurine therapy [33]. Recently, combined chemical and in silico screening using the commercial LOPAC1280 library has identified a series of synthetic, drug-like Nrf2 activators including the experimental PPARγ inhibitor GW9662 (2-chloro-5-nitro-N-phenyl-benzamide) that displayed low toxicity and protected primary human keratinocytes from UVB-induced cell death [35].

Based on the emerging photoprotective potential of small molecule Nrf2 activators and the urgent need for improved Nrf2-directed agents with defined pharmacokinetic and toxicological profile, systemic availability, and established prior clinical performance in human patients, we have focused our attention on tanshinones, a class of medicinal plant-derived phytopharmaceuticals with documented use and efficacy in human patients for antioxidant and anti-inflammatory cardiovascular intervention. Here we have demonstrated that tanshinones are potent Nrf2-activators in cultured human skin keratinocytes and fibroblasts (Figs. 1–4). Our experiments demonstrate that in human skin cells the more potent tanshinones TI and DHT antagonize ubiquitination-dependent turnover of Nrf2 (Fig. 3), thereby extending Nrf2 protein half-life and upregulating Nrf2 transcriptional activity with increased expression of numerous cytoprotective target genes at the mRNA and protein levels (Figs. 1–3). Among the four tested tanshinones, DHT displayed the most pronounced Nrf2-directed effects including Nrf2 transcriptional activation (Fig. 1B) and upregulation of Nrf2 protein half life (Fig. 3C), and was also slightly more effective in raising cellular glutathione and protecting skin cells against solar UV-induced cell death and photooxidative stress (Figs. 3 D–F and 4D–E). However, the structural basis underlying differential potency of Nrf2 activation observed among the four tanshinones tested by us in skin cells remains to be elucidated.

Recently, upregulation of cellular glutathione levels has been identified as an important determinant of Nrf2-dependent cyto- and photoprotective activity, and it has been demonstrated that Nrf2 establishes a glutathione-mediated gradient of UVB-cytoprotection in the epidermis [5]. Indeed, TI and DHT treatment upregulated gene expression underlying glutathione biosynthesis in cultured skin cells and reconstructed human skin (Figs. 2, 3 A, and 4B), and a significant elevation of cellular glutathione levels (between 20 and 40% of untreated controls) was detectable in cultured keratinocytes and fibroblasts exposed to TI and DHT (Figs. 3 D and 4C). However, it remains to be seen if glutathione modulation is the key mechanistic determinant of the photoprotective activity achieved by tanshinone pretreatment of cultured fibroblasts [SSL (Fig. 3E); riboflavin-enhanced UVA (Fig. 3F)], keratinocytes [riboflavin-enhanced UVA (Fig. 4D); SSL (Fig. 4E)] and human reconstructed skin [SSL (Fig. 5)]. Indeed, other factors beyond Nrf2-dependent glutathione upregulation may potentially contribute to tanshinone-induced photoprotection including the modulation of DNA repair and survival signaling pathways all known to be controlled in part by Nrf2, a question to be addressed by future experiments.

In the context of pharmacological modulation of Nrf2 for skin photoprotection, it should be mentioned that Nrf2-activating mutations have been identified in cutaneous squamous cell carcinomas [56]. It has recently been observed that stable overexpression of Nrf2 may result in enhanced resistance of cancer cells to chemotherapeutic agents, and that constitutive activation of Nrf2 function during tumor progression may promote tumorigenicity conferring chemoresistance by upregulation of glutathione, thioredoxin, and drug efflux pathways [57,58]. It has also been shown that prolonged activation of Nrf2 in murine epidermis may cause corneocyte fragility and impaired desquamation [59]. It therefore seems prudent to distinguish between photoprotective strategies that aim at acute versus chronic Nrf2 modulation, and it remains to be seen if Nrf2 activators can be used as safe combinatorial agents together with established sunscreen formulations.

Taken together, our data demonstrate for the first time the feasibility of using tanshinone-based Nrf2-activators as novel skin photoprotectants. In the future, molecular mechanism of action and performance of these agents must be tested more rigorously as a function of solar spectral range in acute and chronic models of human skin photodamage. Moreover, their efficacy as single or combinatorial photoprotective ingredients optimized for targeted topical delivery, photostability, and long-term safety should be evaluated.

Acknowledgments

References

[1] N. Wakabayashi, S.L. Slocum, J.J. Skoko, S. Shin, T.W. Kensler, When NRF2 talks, who's listening? Antioxid. Redox Signal. 13 (2010) 1649–1663.
[2] T. Jiang, Z. Huang, J.Y. Chan, D.D. Zhang, Nrf2 protects against As(III)-induced damage in mouse liver and bladder, Toxicol. Appl. Pharmacol. 240 (2009) 8–14.
[3] T. Suzuki, H. Motohashi, M. Yamamoto, Toward clinical application of the Keap1-Nrf2 pathway, Trends Pharmacol. Sci. 34 (2013) 340–346.

[4] R. Hu, C.L. Saw, R. Yu, A.N. Kong, Regulation of NF-E2-related factor 2 signaling for cancer chemoprevention: antioxidant coupled with antiinflammatory, Antioxid. Redox Signal. 13 (2010) 1679–1698.

[5] M. Schafer, S. Dutsch, U. auf dem Keller, F. Navid, A. Schwarz, D.A. Johnson, J.A. Johnson, S. Werner, Nrf2 establishes a glutathione-mediated gradient of UVB cytoprotection in the epidermis, Genes Dev. 24 (2010) 1045–1058.

[6] C.L. Saw, M.T. Huang, Y. Liu, T.O. Khor, A.H. Conney, A.N. Kong, Impact of Nrf2 on UVB-induced skin inflammation/photoprotection and photoprotective effect of sulforaphane, Mol. Carcinog. 50 (2011) 479–486.

[7] S.B. Kim, R.K. Pandita, U. Eskiocak, P. Ly, A. Kaisani, R. Kumar, C. Cornelius, W.E. Wright, T.K. Pandita, J.W. Shay, Targeting of Nrf2 induces DNA damage signaling and protects colonic epithelial cells from ionizing radiation, Proc. Natl. Acad. Sci. U.S.A. 109 (2012) E2949–2955.

[8] Q. Ma, Role of nrf2 in oxidative stress and toxicity, Annu. Rev. Pharmacol. Toxicol. 53 (2013) 401–426.

[9] Y. Du, N.F. Villeneuve, X.J. Wang, Z. Sun, W. Chen, J. Li, H. Lou, P.K. Wong, D.D. Zhang, Oridonin confers protection against arsenic-induced toxicity through activation of the Nrf2-mediated defensive response, Environ. Health Perspect. 116 (2008) 1154–1161.

[10] A. Lau, S.A. Whitman, M.C. Jaramillo, D.D. Zhang, Arsenic-mediated activation of the Nrf2-Keap1 antioxidant pathway, J. Biochem. Mol. Toxicol. 27 (2013) 99–105.

[11] D.D. Zhang, Mechanistic studies of the Nrf2-Keap1 signaling pathway, Drug Metab. Rev. 38 (2006) 1–21.

[12] T.W. Kensler, N. Wakabayashi, Nrf2: friend or foe for chemoprevention? Carcinogenesis 31 (2010) 90–99.

[13] D.D. Zhang, S.C. Lo, J.V. Cross, D.J. Templeton, M. Hannink, Keap1 is a redox-regulated substrate adaptor protein for a Cul3-dependent ubiquitin ligase complex, Mol. Cell. Biol. 24 (2004) 10941–10953.

[14] A.T. Dinkova-Kostova, W.D. Holtzclaw, T.W. Kensler, The role of Keap1 in cellular protective responses, Chem. Res. Toxicol. 18 (2005) 1779–1791.

[15] J.D. Hayes, M. McMahon, S. Chowdhry, A.T. Dinkova-Kostova, Cancer chemoprevention mechanisms mediated through the Keap1-Nrf2 pathway, Antioxid. Redox Signal. 13 (2010) 1713–1748.

[16] J.D. Adams, R. Wang, J. Yang, E.J. Lien, Preclinical and clinical examinations of Salvia miltiorrhiza and its tanshinones in ischemic conditions, Chin. Med. 1 (2006) 3.

[17] X. Wang, S.L. Morris-Natschke, K.H. Lee, New developments in the chemistry and biology of the bioactive constituents of Tanshen, Med. Res. Rev. 27 (2007) 133–148.

[18] S. Gao, Z. Liu, H. Li, P.J. Little, P. Liu, S. Xu, Cardiovascular actions and therapeutic potential of tanshinone IIA, Atherosclerosis 220 (2012) 3–10.

[19] S. Tao, Y. Zheng, A. Lau, M.C. Jaramillo, B.T. Chau, R.C. Lantz, P.K. Wong, G.T. Wondrak, D.D. Zhang, Tanshinone I Activates the Nrf2-dependent antioxidant response and protects against As(III)-induced lung inflammation in vitro and in vivo, Antioxid. Redox Signal. 19 (2013) 1647–1661.

[20] P. Kullavanijaya, H.W. Lim, Photoprotection, J. Am. Acad. Dermatol. 52 (2005) 937–958. (quiz 959–962).

[21] S. Lautenschlager, H.C. Wulf, M.R. Pittelkow, Photoprotection, Lancet 370 (2007) 528–537.

[22] S.D. Lamore, S. Qiao, D. Horn, G.T. Wondrak, Proteomic identification of cathepsin B and nucleophosmin as novel UVA-targets in human skin fibroblasts, Photochem. Photobiol. 86 (2010) 1307–1317.

[23] S.D. Lamore, S. Azimian, D. Horn, B.L. Anglin, K. Uchida, C.M Cabello, G.T. Wondrak, The malondialdehyde-derived fluorophore DHP-lysine is a potent sensitizer of UVA-induced photooxidative stress in human skin cells, J. Photochem. Photobiol. B 101 (2010) 251–264.

[24] A. Svobodova, J. Vostalova, Solar radiation induced skin damage: review of protective and preventive options, Int. J. Radiat. Biol. 86 (2010) 999–1030.

[25] A. Fourtanier, D. Moyal, S. Seite, UVA filters in sun-protection products: regulatory and biological aspects, Photochem. Photobiol. Sci. 11 (2012) 81–89.

[26] G.T. Wondrak, M.K. Jacobson, E.L. Jacobson, Endogenous UVA-photosensitizers: mediators of skin photodamage and novel targets for skin photoprotection, Photochem. Photobiol. Sci. 5 (2006) 215–237.

[27] A. Hirota, Y. Kawachi, K. Itoh, Y. Nakamura, X. Xu, T. Banno, T. Takahashi, M. Yamamoto, F. Otsuka, Ultraviolet A irradiation induces NF-E2-related factor 2 activation in dermal fibroblasts: protective role in UVA-induced apoptosis, J. Invest. Dermatol. 124 (2005) 825–832.

[28] A.T. Dinkova-Kostova, S.N. Jenkins, J.W. Fahey, L. Ye, S.L. Wehage, K.T. Liby, K.K. Stephenson, K.L. Wade, P. Talalay, Protection against UV-light-induced skin carcinogenesis in SKH-1 high-risk mice by sulforaphane-containing broccoli sprout extracts, Cancer Lett. 240 (2006) 243–252.

[29] A.L. Benedict, E.V. Knatko, A.T. Dinkova-Kostova, The indirect antioxidant sulforaphane protects against thiopurine-mediated photooxidative stress, Carcinogenesis 33 (2012) 2457–2466.

[30] F. Gruber, H. Mayer, B. Lengauer, V. Mlitz, J.M. Sanders, A. Kadl, M. Bilban, R. de Martin, O. Wagner, T.W. Kensler, M. Yamamoto, N. Leitinger, E. Tschachler, NF-E2-related factor 2 regulates the stress response to UVA-1-oxidized phospholipids in skin cells, FASEB J. 24 (2010) 39–48.

[31] F.F. Tian, F.F. Zhang, X.D. Lai, L.J. Wang, L. Yang, X. Wang, G. Singh, J.L. Zhong, Nrf2-mediated protection against UVA radiation in human skin keratinocytes, Biosci. Trends 5 (2011) 23–29.

[32] A. Hirota, Y. Kawachi, M. Yamamoto, T. Koga, K. Hamada, F. Otsuka, Acceleration of UVB-induced photoageing in nrf2 gene-deficient mice, Exp. Dermatol. 20 (2011) 664–668.

[33] S. Kalra, E.V. Knatko, Y. Zhang, T. Honda, M. Yamamoto, A.T. Dinkova-Kostova, Highly potent activation of Nrf2 by topical tricyclic bis(cyano enone): implications for protection against UV radiation during thiopurine therapy, Cancer Prev. Res. Philadelphia 5 (2012) 973–981.

[34] Y. Kawachi, X. Xu, S. Taguchi, H. Sakurai, Y. Nakamura, Y. Ishii, Y. Fujisawa, J. Furuta, T. Takahashi, K. Itoh, M. Yamamoto, F. Yamazaki, F. Otsuka, Attenuation of UVB-induced sunburn reaction and oxidative DNA damage with no alterations in UVB-induced skin carcinogenesis in Nrf2 gene-deficient mice, J. Invest. Dermatol. 128 (2008) 1773–1779.

[35] F. Lieder, F. Reisen, T. Geppert, G. Sollberger, H.D. Beer, U. auf dem Keller, M. Schafer, M. Detmar, G. Schneider, S. Werner, Identification of UV-protective activators of nuclear factor erythroid-derived 2-related factor 2 (Nrf2) by combining a chemical library screen with computer-based virtual screening, J. Biol. Chem. 287 (2012) 33001–33013.

[36] S.D. Lamore, G.T. Wondrak, UVA causes dual inactivation of cathepsin B and L underlying lysosomal dysfunction in human dermal fibroblasts, J. Photochem. Photobiol. B 123 (2013) 1–12.

[37] X.J. Wang, Z. Sun, W. Chen, Y. Li, N.F. Villeneuve, D.D. Zhang, Activation of Nrf2 by arsenite and monomethylarsonous acid is independent of Keap1-C151: enhanced Keap1-Cul3 interaction, Toxicol. Appl. Pharmacol. 230 (2008) 383–389.

[38] Z. Sun, S. Zhang, J.Y. Chan, D.D. Zhang, Keap1 controls postinduction repression of the Nrf2-mediated antioxidant response by escorting nuclear export of Nrf2, Mol. Cell. Biol. 27 (2007) 6334–6349.

[39] S.D. Lamore, G.T. Wondrak, Zinc pyrithione impairs zinc homeostasis and upregulates stress response gene expression in reconstructed human epidermis, Biometals 24 (2011) 875–890.

[40] D.D. Zhang, M. Hannink, Distinct cysteine residues in Keap1 are required for Keap1-dependent ubiquitination of Nrf2 and for stabilization of Nrf2 by chemopreventive agents and oxidative stress, Mol. Cell. Biol 23 (2003) 8137–8151.

[41] K. Sato, H. Taguchi, T. Maeda, H. Minami, Y. Asada, Y. Watanabe, K. Yoshikawa, The primary cytotoxicity in ultraviolet-a-irradiated riboflavin solution is derived from hydrogen peroxide, J. Invest. Dermatol. 105 (1995) 608–612.

[42] G.T. Wondrak, M.J. Roberts, M.K. Jacobson, E.L. Jacobson, 3-Hydroxypyridine chromophores are endogenous sensitizers of photooxidative stress in human skin cells, J. Biol. Chem. 279 (2004) 30009–30020.

[43] A. Van Laethem, S. Claerhout, M. Garmyn, P. Agostinis, The sunburn cell: regulation of death and survival of the keratinocyte, Int. J. Biochem. Cell. Biol. 37 (2005) 1547–1553.

[44] F. Bernerd, D. Asselineau, An organotypic model of skin to study photodamage and photoprotection in vitro, J. Am. Acad. Dermatol. 58 (2008) S155–159.

[45] L. Marrot, J.R. Meunier, Skin DNA photodamage and its biological consequences, J. Am. Acad. Dermatol. 58 (2008) S139–148.

[46] F.P. Gasparro, Sunscreens, skin photobiology, and skin cancer: the need for UVA protection and evaluation of efficacy, Environ. Health Perspect. 108 (Suppl. 1) (2000) 71–78.

[47] G.T. Wondrak, Let the sun shine in: mechanisms and potential for therapeutics in skin photodamage, Curr. Opin. Invest. Drugs 8 (2007) 390–400.

[48] M.S. Matsui, A. Hsia, J.D. Miller, K. Hanneman, H. Scull, K.D. Cooper, E. Baron, Non-sunscreen photoprotection: antioxidants add value to a sunscreen, J. Invest. Dermatol. Symp. Proc. 14 (2009) 56–59.

[49] A.T. Dinkova-Kostova, Phytochemicals as protectors against ultraviolet radiation: versatility of effects and mechanisms, Planta Med. 74 (2008) 1548–1559.

[50] M.S. Baliga, S.K. Katiyar, Chemoprevention of photocarcinogenesis by selected dietary botanicals, Photochem. Photobiol. Sci. 5 (2006) 243–253.

[51] F. Afaq, H. Mukhtar, Botanical antioxidants in the prevention of photocarcinogenesis and photoaging, Exp. Dermatol. 15 (2006) 678–684.

[52] J.A. Nichols, S.K. Katiyar, Skin photoprotection by natural polyphenols: anti-inflammatory, antioxidant and DNA repair mechanisms, Arch. Dermatol. Res. 302 (2010) 71–83.

[53] G.T. Wondrak, C.M. Cabello, N.F. Villeneuve, S. Zhang, S. Ley, Y. Li, Z. Sun, D.D. Zhang, Cinnamoyl-based Nrf2-activators targeting human skin cell photo-oxidative stress, Free Radic. Biol. Med. 45 (2008) 385–395.

[54] Y.C. Hseu, C.W. Chou, K.J. Senthil Kumar, K.T. Fu, H.M. Wang, L.S. Hsu, Y.H. Kuo, C.R. Wu, S.C. Chen, H.L. Yang, Ellagic acid protects human keratinocyte (HaCaT) cells against UVA-induced oxidative stress and apoptosis through the upregulation of the HO-1 and Nrf-2 antioxidant genes, Food Chem. Toxicol. 50 (2012) 1245–1255.

[55] S.E. Dickinson, T.F. Melton, E.R. Olson, J. Zhang, K. Saboda, G.T. Bowden, Inhibition of activator protein-1 by sulforaphane involves interaction with cysteine in the cFos DNA-binding domain: implications for chemoprevention of UVB-induced skin cancer, Cancer Res. 69 (2009) 7103–7110.

[56] Y.R. Kim, J.E. Oh, M.S. Kim, M.R. Kang, S.W. Park, J.Y. Han, H.S. Eom, N.J. Yoo, S.H. Lee, Oncogenic NRF2 mutations in squamous cell carcinomas of oesophagus and skin, J. Pathol. 220 (2010) 446–451.

[57] X.J. Wang, Z. Sun, N.F. Villeneuve, S. Zhang, F. Zhao, Y. Li, W. Chen, X. Yi, W. Zheng, G.T. Wondrak, P.K. Wong, D.D. Zhang, Nrf2 enhances resistance of cancer cells to chemotherapeutic drugs, the dark side of Nrf2, Carcinogenesis 29 (2008) 1235–1243.

[58] D.D. Zhang, The Nrf2-Keap1-ARE signaling pathway: the regulation and dual function of Nrf2 in cancer, Antioxid. Redox Signal. 13 (2010) 1623–1626.

[59] M. Schafer, H. Farwanah, A.H. Willrodt, A.J. Huebner, K. Sandhoff, D. Roop, D. Hohl, W. Bloch, S. Werner, Nrf2 links epidermal barrier function with antioxidant defense, EMBO Mol. Med. 4 (2012) 364–379.